Colloid and Interface Science Communications 57 (2023) 100747

Contents lists available at ScienceDirect

Colloid and Interface Science Communications

journal homepage: www.elsevier.com/locate/colcom

Rapid Communication

Photocatalytic and antibacterial performance of β-cyclodextrin-TiO_2 nanoparticles loading sorbic and benzoic acids

Leire Goñi-Ciaurriz [a], Pablo Rosas-Val [b], Carlos Gamazo [b], Itziar Vélaz [a,*]

[a] Department of Chemistry, School of Sciences, University of Navarra, 31008 Pamplona, Spain
[b] Department of Microbiology & Parasitology, School of Medicine, University of Navarra, 31008 Pamplona, Spain

ARTICLE INFO

Keywords:
β-Cyclodextrin-TiO_2 nanoparticles
Sorbic acid
Benzoic acid
Antibacterial activity
Photocatalytic activity

ABSTRACT

TiO_2 nanoparticles (NPs) have been modified with β-cyclodextrin (βCD)-food preservative complexes. The susceptibility of *Escherichia coli* and *Staphylococcus aureus* to TiO_2 NPs, sorbic acid (SA), benzoic acid (BA), and β-Cyclodextrin-TiO_2 NPs including SA or BA, was studied. At 0.5 mg mL^{-1}, TiO_2 NPs were more effective in the inhibition of bacterial growth than modified-TiO_2 NPs, achieving 71% inhibition rate. At the higher concentration of 3 mg mL^{-1} there were no significant differences between treatments, being all of them highly effective reaching 90% inhibition. Higher treatment-doses were related to slower growth rates. Flow cytometry findings suggested efficient NPs interaction with bacteria, being more noticeable in the case of TiO_2 NPs. Regarding the photocatalytic activity, under 0.600 mW cm^{-2} irradiation, TiO_2 NPs reached 95% methylene-blue dye degradation after 150 min, while βCD-TiO_2 NPs showed 3-times lower kinetic constant. Overall results suggest potential application of the new systems in active packages to protect food from microbial spoilage.

1. Introduction

Currently consumer demands for unprocessed, high-quality, safe, and sustainable foods have led to the development of advanced packaging: smart and active films, and edible coatings. Active packaging interacts with food by absorbing or releasing substances, which help to extend foods shelf-life, and maintain its safety and quality. Several additives as antimicrobials, antioxidants, and gas scavenging systems are the most recurring [1].

Nanoparticles (NPs) with antimicrobial activity are being widely used in the development of active packaging. As part of composite functional films, they contribute to protect food from spoilage microorganisms, and ensure food safety and freshness [2]. In particular, TiO_2 NPs, as an inert and highly stable photocatalyst have many advantages including low cost and toxicity, and antibacterial properties against a wide range of microorganisms [3]. The antibacterial activity of TiO_2 is mainly attributed to the generation of reactive oxygen species (ROS) such as hydroxyl radicals (OH•) and superoxide radicals (O_2^-) upon UV light irradiation (< 386 nm) [4]. TiO_2 has received GRAS (Generally Regarded as Safe) status by the American Food and Drug Administration (FDA) to be used as food additive [5]. However, recent concerns regarding the safety of nanomaterials in food packaging has led to a comprehensive study on the migration properties of TiO_2 from active films. Several studies have evidenced that the amount of TiO_2 migrated from polymeric films into food simulants was negligible, and showed no toxic effects on human colon cells and intestinal bacteria [6]. The inclusion of TiO_2 NPs in polymer composite packages has many performances. In addition to the strong antimicrobial feature [7], researchers have demonstrated an improvement on the mechanical and barrier properties of polymeric materials [8]. Additionally, TiO_2 NPs can facilitate polymer degradation under light irradiation, thus easing the packages disposal after their life-use [9]. However, in the development of such packaging materials, maintaining the inhibitory effect of the active compound on microbial growth during a long time is still a challenge. In order to obtain a system that enables slow and continuous migration of antimicrobial agents onto the food surface, TiO_2 NPs were modified with cyclodextrins (CDs), and the system was proposed as a useful nanocarrier for the sustained delivery of food preservatives in a previous work [10]. CDs are cyclic oligosaccharides made of α-(1, 4) linked glucopyranose units. There are three types of natural cyclodextrins: αCD, βCD, and γCD consisting of 6, 7 or 8 glucose units, respectively; rearranged on a truncated cone shape that allows formation of stable inclusion complexes with several molecules [11]. CDs themselves do not have antibacterial activity. Instead, in food packaging industry

* Corresponding author.
E-mail address: itzvelaz@unav.es (I. Vélaz).

https://doi.org/10.1016/j.colcom.2023.100747
Received 7 April 2023; Received in revised form 6 October 2023; Accepted 13 October 2023
Available online 24 October 2023

they are mainly employed to encapsulate and steadily release antimicrobials and antioxidants, to provide them protection against loss and heat during the fabrication of the film, and to retain unpleasant flavours and odours. Also, as biodegradable compounds, they improve the biodegradability of the carrier polymer to acquire environmentally friendly packages [12]. The CD-TiO_2 system can be obtained by direct adsorption of the CD onto the surface of TiO_2; or including a cross-linker able to attach hydroxyl groups of the catalyst and the macrocycle. In the purpose of including an active compound within the CD cavity, the second option is more convenient, since the spacer prevents the degradation of the active by TiO_2 [10]. Among food preservatives, sorbic acid (SA) and benzoic acid (BA) are widely used to maintain or improve food quality and safety. SA and BA considered as non-harmful to human substances are potential inhibitors against fungi and some bacteria [13,14].

In order to assess the effectiveness of TiO_2 photocatalytic processes, the disappearance of organic dyes is usually monitored, where even a slight modification in their structure can lead to their degradation. As an example, methylene blue (MB) is an organic dye commonly used as a pollutant model to assess the photocatalytic capacity of metallic NPs [15]. Conversely, when it is about degrading microorganisms, the objective is to inactivate cells, resulting in cellular death by compromising the integrity of their bacterial walls and oxidizing their intracellular components. Interestingly, both the decomposition of organic matter and the eradication of microorganisms through photocatalysis seem to follow similar mechanisms, which involve the excitation, recombination, and trapping of electron-hole pairs, as well as the attach or ROS. The OH· radical, generated by irradiated TiO_2, has been identified as the primary oxidative species responsible for the mineralization of organic chemicals and biological cells. On the basis of these analogous mechanisms, it is plausible to assume that there may be a correlation between the degradation of organic matter and the inactivation of microorganisms in the photocatalytic process. Previous studies have analyzed the relationship between the photocatalytic and antibacterial activities of different nanomaterials [16]. Table 1 collects a recent comparison between the photocatalytic degradation of dyes and the antibacterial activity of TiO_2-based nanomaterials against different bacteria.

In this context, it has been hypothesized that the inclusion of sorbic acid (SA) and benzoic acid (BA) in the polyfunctional system based on TiO_2 NPs modified with βCD can reinforce and extend the inhibitory effect on the microbial growth over time as a result of the controlled release of the food preservatives from the CD. Based on this approach, growth susceptibility of *Escherichia coli* and *Staphylococcus aureus* cells at various concentrations of TiO_2 NPs, SA, BA, βCD-SA-TiO_2 NPs and βCD-BA-TiO_2 NPs was evaluated. The physical status of *E. coli* and *S. aureus* and NPs uptake were also investigated by flow cytometry analysis. In addition, it has also been hypothesized that the antibacterial activity of the synthesized NPs is directly related to their photocatalytic activity. Therefore, studies on photocatalytic capacity of unmodified and modified TiO_2 NPs were also performed. The system is intended to be used as a novel approach to develop active packaging.

2. Materials and methods

2.1. Materials

Sorbic acid (SA; 99% purity), Benzoic acid (BA; 99.9%) and Titanium (IV) oxide nanoparticles (TiO_2 NPs; 99.5% purity, 21 nm average size and $\rho = 4.26\ g \bullet cm^{-3}$, ST Louis, MO, USA) were provided by Sigma-Aldrich. β-Cylodextrin (βCD; 12.5% water content) was manufactured by Roquette (Laisa España S.A.). Tryptic soy agar (TSA) and tryptic soy broth (TSB) were provided by Scharlau. Phophate-buffered saline (PBS) and PBS-Bovine serum albumin 0.1% *w/v* (PBS-BSA; A4503), and 5(6)-Carboxy-2′,7′-dichlorofluorescein diacetate (CDCF; 21,884) were procured by Sigma-Aldrich.

2.2. Bacteria

Escherichia coli ATCC 25922 (*E. coli*) and *Staphylococcus aureus* ATCC 43300 (*S. aureus*) were tested. The strains were stored at −20 °C prior to use. During the experiment cultures were grown at 37 °C on tryptone soy agar plates (064PA0031I, Scharlab) for 24 h, and then kept at 4 °C. *E. coli* and *S. aureus* were subjected to growth curve measurements and flow cytometry analysis.

2.3. Growth curves

Firstly, βCD-TiO_2 NPs were obtained by crosslinking with hexamethylene diisocyanate (HMDI) as linear spacer under a two stages reaction. In a first step, HMDI was covalently joined to the surface of TiO_2 NPs in dimethylformamide (DMF) solution under nitrogen atmosphere at 100 °C during 72 h (HMDI-TiO_2). After that, CDs were attached to the HMDI by mixing the product of the last step with 9 g of previously dried βCD. The reaction proceeded under nitrogen atmosphere and stirring for 48 h at 100 °C. The product was centrifuged at 8000 rpm for 30 min and washed three times with methanol. Lastly, βCD-HMDI-TiO_2 NPs were let to dry completely at 50 °C in an oven to obtain the solid product. The detailed mechanism on the modification of TiO_2 NPs surface with βCD, and the characterization of the obtained system was previously described [10,21].

Growth kinetic assays and cytotoxicity analyses were performed by broth dilution method, measuring the change in the optical density (OD) of bacterial suspension from 0 to 72 h at time intervals of 60 min using a Bioscreen C automated spectrophotometer (Thermo Labsystems). The OD was measured with a wideband in the range of 420–580 nm ($OD_{420–580}$) as this filter is less sensitive to color changes than other filters, therefore the results are not affected that much by change of color of growth medium and are more precise. In the present study, as growth of different bacterial strains were studied and the medium employed has

Table 1
Comparison of photocatalytic and antibacterial activities of different nanomaterials.

Nanomaterial	Model dye (conc)	Photocatalytic degradation (%)	Dose of catalyst/ time/light	Tested organism	Growth inhibition (%) (time)	Dose of catalyst	Ref.
TiO_2 NPs 0.2% Mn-doped TiO_2 NPs	MB (3 μg mL^{-1})	75 96	1 mg mL^{-1} / 60 min/visible	*E.coli*	99 (30 min) 99.9 (30 min)	2.5 mg mL^{-1}	[17]
0.8% TiO_2-doped CS/AC NPs	Rose Bengal (7.9 μg mL^{-1})	91.9	1 mg mL^{-1} / 120 min/UV	*E. coli* *P. aeruginosa* *B. subtilis* *S. aureus*	21.8 93.6 96.5 96.3	1 mg mL^{-1}	[18]
TiO_2 nanocomposite films	MB (6.4 μg mL^{-1})	54	−/60 min/UV	*E. coli, S.aureus*	99.9 (60 min)	–	[19]
10% Zr-doped TiO_2 nanomembranes	MB (10 μg mL^{-1})	94.3	−/300 min/UV	*E. coli* *S. aureus*	96 (20 min) 97.8 (20 min)		[20]

*CS: Sustainable chitosan; AC: Activated charcoal.

a strong change of color when logarithmic phase starts, the wideband of 420–580 nm was chosen.

The initial concentration of the strains was adjusted to $5.5 \bullet 10^5$ CFUs mL^{-1} in TSB medium. The standard stock solutions of TiO_2 NPs were prepared in TSB medium. Aliquots of 200 μL of *E. coli* ATCC 25922 or *S. aureus* ATCC 43300 suspensions and different concentrations (250, 500, 1000 and 3000 μg mL^{-1}) of the studied systems (SA, BA, unmodified and modified TiO_2 NPs including food preservatives) were added to each well in a 96-well plate, separately. The final volume of each well on the microplate was adjusted to 300 μL with TSB medium. The microplates were incubated in the spectrophotometer at 37 °C under continuous stirring for 72 h. Figures have been drawn up to 48 h, since the stationary phase of the bacterial growth was already reached at this time. To determine the growth kinetic parameters, bacterial growth curves were fitted to a modified Gompertz equation, commonly used empirical model [22]:

$$OD_t = B^* exp(-exp(e^* \mu^* (L-t)/B+1)) \quad (1)$$

where t is the time in hours passed since inoculation, OD_t is the optical density (range of 420–580 nm) at time t, μ is the maximum growth rate (ΔOD_t/h), L is the time in hours at the end of lag stage, and B is the increase in $OD_{420–580}$ from inoculation to the stationary phase.

All experiments were performed in triplicate. Kinetic growth parameters μ, L and D (maximum $OD_{420–580}$ h^{-1} in the stationary phase) were obtained using Origin 2016 software. Statistical analysis was performed using analysis of variance (ANOVA) by Origin 2016. Multiple comparisons means were performed using Tukey's Studentized Range test at a significance level of 5% ($P < 0.05$), and $P < 0.01$ showed highly significant difference.

2.4. Bacterial viability assessed by flow cytometry

Strains of *E. coli* ATCC 25922 and *S. aureus* ATCC 43300 were grown in TSA at 37 °C for 24 h. Then, isolated colonies were suspended in prewarmed PBS. Then, dilutions in PBS were made to reach a final bacterial concentration of $5.5 \bullet 10^5$ CFUs mL^{-1}. Both bacterial species were incubated with different treatments and varying concentrations of NPs (TiO_2, βCD-BA-TiO_2, βCD-SA-TiO_2, at 0.5 mg vs. 3 mg) at 37 °C for 12 h, with constant shaking (100 rpm).

After the incubation period, cells were harvested and washed twice in prewarmed PBS with 0.1% wt/v BSA. Then, bacteria were incubated with 50 μM CDCF at 37 °C for 15 min in the dark. Cells were washed again twice with PBS-BSA, and were collected for flow cytometry analysis. For each sample, triplicates were made. Pasteurized-inactivated bacteria (65 °C, 30 min) were used as negative control.

Flow analysis was conducted on an Attune cytometer (Applied Biosystems) and assessed for the percentage of fluorescent staining. Firstly, size and internal complexity were determined for sample identification by forward-scatter(ed) light (FSC) and side-scatter(ed) light (SSC), respectively. Once the bacterial population was selected the metabolic activity (live bacteria) was determined by CDCF fluorescence intensity. CDCF is commonly employed to measure the formation of reactive oxygen species (ROS) in bacteria.

All experiments were performed in triplicate. Statistical analysis was conducted using analysis of variance (ANOVA) by Origin 2016. Multiple comparisons means were performed using Tukey's Studentized Range test at a significance level of 5% ($P < 0.05$).

2.5. Photocatalytic activity

In order to study the possible dependence of the NPs antibacterial activity on their photocatalytic capacity, photocatalytic assays were performed. The photocatalytic activity of the unmodified and βCD-food preservative-TiO_2 NPs was evaluated by the photodegradation of Methylene Blue (MB) dye in aqueous solution at room temperature (25 °C). The photocatalysis experiments were conducted using a high-intensity fluorescent Sylvania BLB-T8/F15W lamp as the light source, emitting UV-A light with a spectral peak at 367 nm. This wavelength range was chosen to align with the activation spectrum of the photocatalyst, TiO_2. In the experiment, 50 mg of NPs were used as catalyst, and dispersed in 150 mL of MB solution (10^{-5} mol L^{-1}). Then, the solutions were stirred for 30 min in dark to bring equilibrium condition following the adsorption-desorption process. At this time, an aliquot was extracted and considered as initial concentration of dye, C_0 ($t = 0$). The suspensions were then subjected to two different UV light irradiation intensities: 0.600 and 0.200 mW cm^{-2}. Serial aliquots were obtained at fixed time intervals for further analysis. The concentration of the dye in the solution was determined by UV–Vis spectroscopy following the absorbance at $\lambda_{max} = 664$ nm. In addition, the degradation of MB was measured without UV irradiation, as a control. In this case, small reduction in the absorption intensity of MB was observed, meaning that there was a slight degradation of the dye by all the catalysts, which is valid for all metal-doped NPs [23]. Serial aliquots were obtained at fixed time intervals for further analysis.

The kinetic of the photocatalytic degradation rate of MB was assumed to follow the Langmuir-Hinshelwood kinetic model, according to the following equation:

$$ln\frac{C_t}{C_0} = -kt \quad (2)$$

where C_t is the dye concentration at a time t, C_0 represents the initial concentration of dye at adsorption-desorption equilibrium, and k is a pseudo first order rate constant (min^{-1}). Curves on MB degradation were fitted to Eq. (2) to determine the kinetic constants using Origin 2016 software.

3. Results and discussion

The linkage between βCD-HMDI-TiO_2 NPs was confirmed using Fourier transform infrared spectroscopy (FTIR) and Thermogravimetric analysis (TGA) techniques. The three times washing and centrifuging (8000 rpm, 30 min) steps carried out at the end of the synthesis, ensure the bonding between the molecules, and allow to discard the adsorption of any compound to the NPs surface. Detailed characterization of the βCD-TiO_2 system can be found in the Supplementary Material section (**Fig. A.1**), which provides a comprehensive account of the analyses previously reported [24]. In addition, the encapsulation and further delivery of sorbic acid (SA) and benzoic acid (BA) food preservatives in βCD-TiO_2 NPs was reported. In this work, a fast initial release of both food preservatives was observed due to their adsorption to the cyclodextrin modified TiO_2 NPs surface. After a while, the delivery slowed down as the encapsulated SA and BA molecules released from the cyclodextrin.

3.1. Bacterial growth curves

A total of 72 growth curves were obtained for each examined strain by measuring the change in the optical density of bacterial suspensions between 420 and 580 nm ($OD_{420–580}$) from 0 to 72 h. Using the normalized mean $OD_{420–580}$ values kinetic growth parameters were determined for each bacteria using modified-Gompertz equation (1). **Figs. 1** and **2** show the growth curves under exposition to different nanosystems (TiO_2, βCD-SA-TiO_2 and βCD-BA-TiO_2 NPs) and several concentrations (250, 500, 1000 and 3000 μg mL^{-1}) of *E. coli* and *S. aureus* strains, respectively.

The estimated growth kinetic parameters (lag phase, maximum growth rate and maximum $OD_{420–580}$ in the stationary stage) are compiled in **Tables 2** and **3**. Both *E. coli* and *S. aureus* growth curves were well fitted ($R^2 > 0.90$) to the modified-Gompertz model (Eq.1), except the ones in presence of 1 and 3 mg mL^{-1} TiO_2 NPs. In these cases,

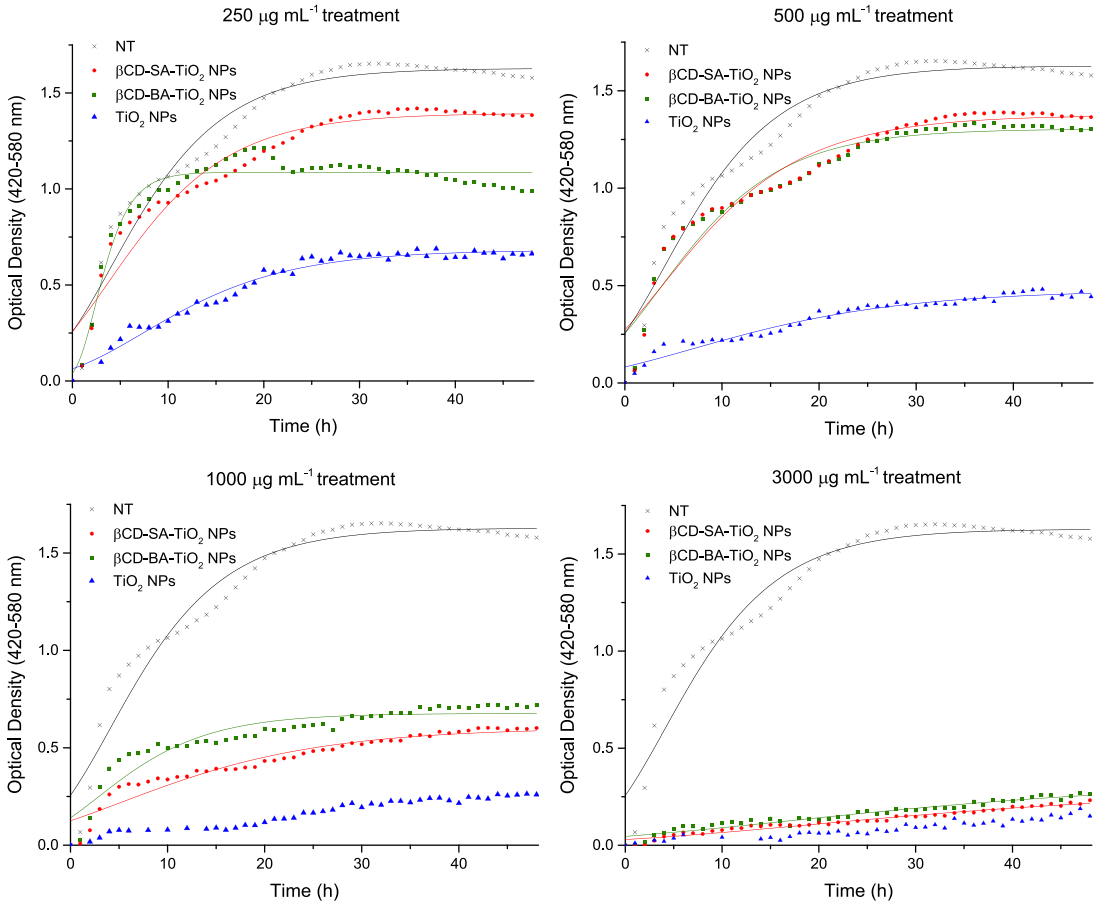

Fig. 1. Growth curves of *Escherichia coli* ATCC 25922 incubated in TSB at 37 °C without treatment (NT), and exposed to various concentrations (250, 500, 1000 and 3000 μg mL^{-1}) of β-Cyclodextrin-Benzoic acid-TiO_2 Nanoparticles (βCD-BA-TiO_2 NPs), β-Cylodextrin-Sorbic acid-TiO_2 Nanoparticles (βCD-SA-TiO_2 NPs) and TiO_2 NPs.

the inhibition growth was higher than 85% regarding the control without antimicrobials, thus they did not fit the model. The growth of *E. coli* ATCC 25922 and *S. aureus* ATCC 43300 was negatively affected in the presence of TiO_2, βCD-SA-TiO_2 and βCD-BA-TiO_2 NPs. Furthermore, exposure to increasing concentrations of the antimicrobials (ranged from 0.25 to 3 mg mL^{-1}) decreased the viability of both bacteria.

Specifically, in the case of *E. coli*, TiO_2 NPs were more active, achieving 59% and 71% growth reduction at 0.25 and 0.5 mg mL^{-1} concentrations, respectively. The modification of TiO_2 with βCD-SA and βCD-BA showed significant ($P < 0.05$) reduction on the antibacterial activity of the NPs at the lower concentrations. Under 0.25 and 0.5 mg mL^{-1} βCD-TiO_2 treatments, the viability of *E. coli* was quite similar. The mean growth inhibition reached was 23%, with non-significant differences depending on the food preservative included in the NPs (SA or BA). At the concentration of 3 mg mL^{-1} there were no significant differences between treatments, all of them were highly effective reducing the bacteria growth in almost 90%.

On the other hand, a higher maximum growth rate (μ) was observed in the control without antimicrobials than in the treated samples. In general, μ decreased as the amount of NPs increased, and TiO_2 treatment displayed the lowest μ rates of microbial growth. So on, higher inhibition of bacterial growth was associated with lower growth rates, μ. However, no trend was observed for the lag phase, L, upon increasing the concentration of antimicrobials. Only in the case of βCD-SA-TiO_2 NPs, shorter lag phases were observed as the concentration rose, which would imply that in the presence of this antimicrobial *E. coli* begins to grow rapidly. A prior study have experienced a similar phenomenon on a different enterobacterial specie, *Cronobacter sakazakii*, treated with different biocides [25].

At high doses of treatment, the inhibition of bacteria reaches almost 100%; the curves lose their exponential growth and become linear, so the fitting does not converge or, in case of convergence, it does so with large error values. However, as explained above, the lag phase (L) is not strongly dependent on the treatment dose and does not follow a clear trend. Triplicate measurement of lag phase values were quite similar, and close to zero. When the values are so small, it is common to find relative errors higher than the actual measurement itself. For this reason, in **Figs. 1 and 2**, and in Tables 2, 3, **A.1** and **A.2**, some fitting lines and kinetic parameters at 1000 and 3000 μg mL^{-1} have been removed, respectively.

Regarding *S. aureus* viability, TiO_2 NPs were highly toxic at the concentration of 0.5 mg mL^{-1}, reaching 67% growth inhibition. The βCD-food preservative-TiO_2 NPs were found effective in the inhibition of ATCC 43300 at the higher dose of 1 mg mL^{-1} (53% and 68% for BA and SA systems, respectively). Also for this strain, non-significant differences were observed depending on the food preservative included in the NPs. Moreover, the highest maximum growth rate (μ) was displayed by the sample without antimicrobials. A relation was observed between the growth rate and the inhibition of bacterial growth; higher growth inhibitions were accompanied by slower growth rates. Also in this case, no trend was exhibited by the lag phase.

For comparative purposes, the growth curves of both strains in presence of free food preservatives (SA and BA) were obtained (see **Supplementary material Fig. A.2, A.3 and Tables A.1, A.2**). The same concentrations studied for NPs (0.25, 0.5, 1, 3 mg mL^{-1}) were employed, as well as the concentrations of food preservatives encapsulated in the

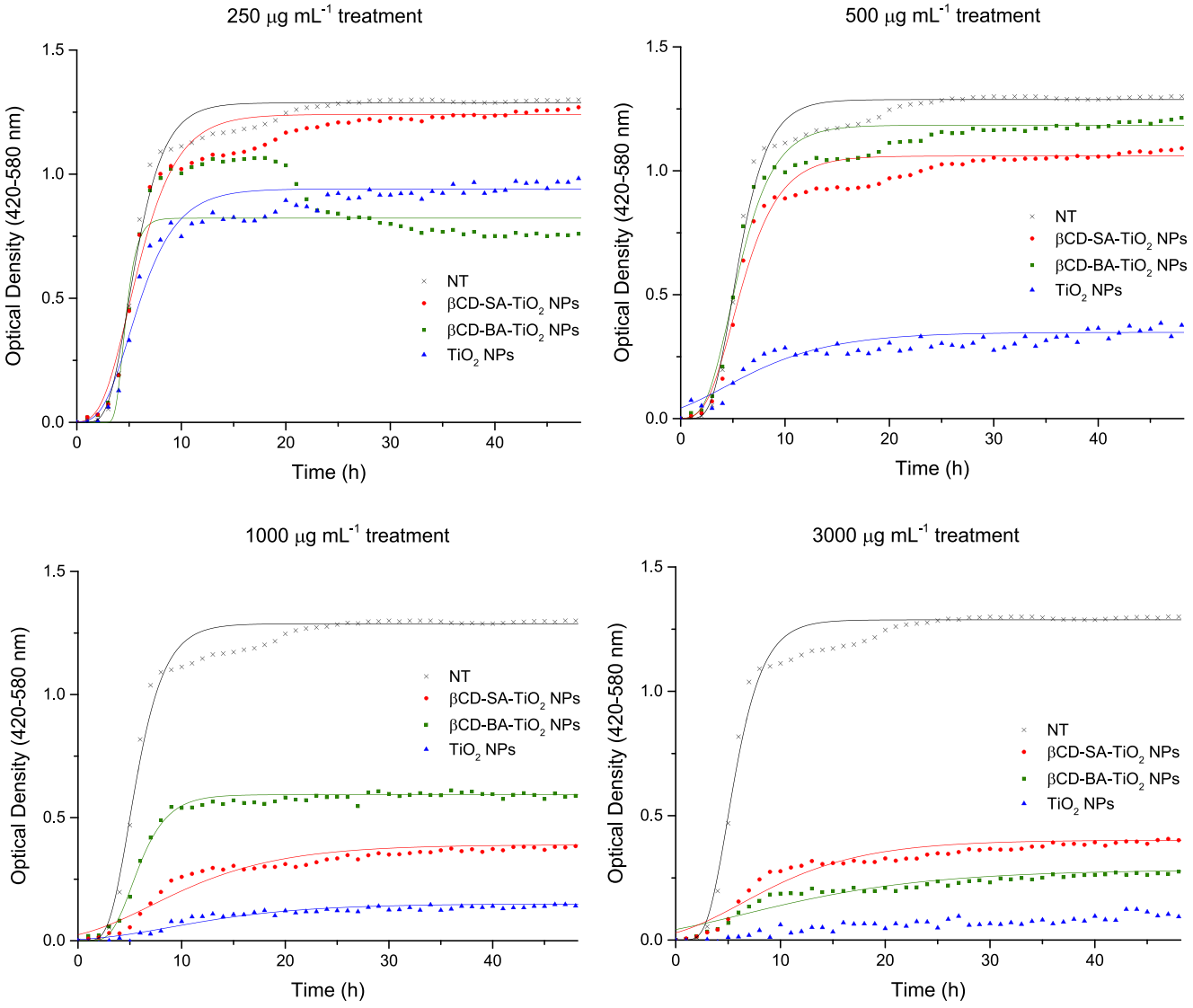

Fig. 2. Growth curves of *Staphylococcus aureus* ATCC 43300 incubated in TSB at 37 °C without treatment (NT), and exposed to various concentrations (250, 500, 1000 and 3000 μg mL^{-1}) of β-Cyclodextrin-Benzoic acid-TiO_2 Nanoparticles (βCD-BA-TiO_2 NPs), β-Cylodextrin-Sorbic acid-TiO_2 Nanoparticles (βCD-SA-TiO_2 NPs) and TiO_2 NPs.

βCD-TiO_2 NPs (3.5 μg mL^{-1} food preservative is the amount present in 500 μg mL^{-1} of βCD-food preservative-TiO_2 NPs; 7 μg mL^{-1} in 1000 μg mL^{-1}; 21 μg mL^{-1} in 3000 μg mL^{-1} modified-TiO_2 NPs). It was observed that the toxicity of SA and BA against *E. coli* and *S. aureus* was lower than that of TiO_2 NPs, being highly effective only at the concentration of 3 mg mL^{-1}. As observed in **Fig. A.2.** and **A.3.**, the antibacterial effect of SA and BA is similar. Furthermore, at the concentration of 1000 μg mL^{-1} it can be observed that *S. aureus* is slightly more susceptible than *E. coli* to weak acids. Gram-negative bacteria have an outer membrane that serves as a barrier to many substances, that is the reason why they are typically less susceptible to weak acids than Gram-positive ones [26]. Other studies have exhibited the resistance of some foodborne pathogenic bacteria, as *E. coli*, against organic acids, such as SA and BA and their derived salts [27]. In fact, yeasts and fungi have been shown to be more susceptible to the toxicity of these food preservatives. Therefore, it would be interesting in the future to analyse the antimicrobial activity of the modified NPs also against these types of microorganisms. To end, antimicrobial capacity of all weak acid food preservatives is highly increased at acidic pH [28].

A previous study demonstrated the release capacity of food preservatives from βCD-TiO_2 NPs [10]. Their lower antibacterial activity regarding the unmodified TiO_2 may have different explanations. Firstly, the amount of food preservatives loaded in βCD-TiO_2 NPs is quiet low. Moreover, βCD coverage around TiO_2 NPs surface may hindrance their interaction with bacteria, and thus their antibacterial activity. βCD-food preservative-TiO_2 NPs were effective against *E. coli* and *S. aureus*, but relatively high concentrations were required to inhibit bacterial growth. On the other hand, the antibacterial effect of the NPs when incorporated as an additive into different polymeric binders may differ depending on the type of binder used [29]. And also, the controlled release of the food preservatives from the polymeric matrix may extend over time the antibacterial effect of the NPs.

3.2. Flow cytometry analysis

The results obtained by flow cytometry, also revealed a negative dose-dependent effect of unmodified and modified TiO_2 NPs on the viability of *E. coli* ATCC 25922 and *S. aureus* ATCC 43300. In order to examine the accumulation of NPs in both bacteria, and their physical status, cell size and intracellular complexity were determined by FSC and SSC, respectively. Fig. 3 shows the acquired histograms on SSC intensity (log scale) for *E. coli* and *S. aureus* under the several treatments

Table 2
Growth kinetic parameters of *Escherichia coli* ATCC 25922 incubated in TSB at 37 °C without treatment, and exposed to various concentrations of nanoparticles as indicated. Lag phase (L; hours), maximum growth rate (μ; $\Delta OD_{420-580}\ h^{-1}$) and maximum $OD_{420-580}$ (h^{-1}) in the stationary phase (D). Data show mean ± SD; $n = 3$.

Nanoparticles	Concentration of NPs (μg mL^{-1})	Growth kinetic parameters		
		L	μ	D
Without NPs		−2.572 ± 0.707	0.090 ± 0.006	1.652 ± 0.005
TiO_2	250	−1.163 ± 0.659	0.029 ± 0.002	0.683 ± 0.091
	500	−5.448 ± 1.192	0.014 ± 0.001	0.478 ± 0.080
	1000	–	0.016 ± 0.004	0.261 ± 0.075
	3000	–	0.007 ± 0.002	0.156 ± 0.064
βCD-SA-TiO_2	250	−3.437 ± 0.845	0.071 ± 0.006	1.420 ± 0.032
	500	−4.271 ± 1.033	0.062 ± 0.005	1.389 ± 0.037
	1000	−6.497 ± 1.521	0.019 ± 0.002	0.603 ± 0.195
	3000	−4.240 ± 1.259	0.005 ± 0.001	0.220 ± 0.098
βCD- BA-TiO_2	250	0.389 ± 0.296	0.197 ± 0.019	1.126 ± 0.048
	500	−3.655 ± 0.893	0.067 ± 0.006	1.292 ± 0.072
	1000	−3.522 ± 1.117	0.039 ± 0.004	0.713 ± 0.124
	3000	−7.500 ± 1.669	0.005 ± 0.001	0.259 ± 0.098

Table 3
Growth kinetic parameters of *Staphylococcus aureus* ATCC 43300 incubated in TSB at 37 °C without treatment, and exposed to various concentrations of nanoparticles as indicated. Lag phase (L; hours), maximum growth rate (μ; $\Delta OD_{420-580}\ h^{-1}$) and maximum $OD_{420-580}$ (h^{-1}) in the stationary phase (D). Data show mean ± SD; $n = 3$.

Nanoparticles	Concentration of NPs (μg mL^{-1})	Growth kinetic parameters		
		L	μ	D
Without NPs		3.005 ± 0.196	0.250 ± 0.017	1.349 ± 0.006
TiO_2	250	2.439 ± 0.350	0.137 ± 0.013	1.028 ± 0.122
	500	−1.511 ± 1.311	0.022 ± 0.003	0.444 ± 0.200
	1000	1.621 ± 1.041	0.008 ± 0.001	0.177 ± 0.064
	3000	–	–	0.131 ± 0.021
βCD-SA-TiO_2	250	2.369 ± 0.307	0.179 ± 0.015	1.322 ± 0.102
	500	2.460 ± 0.325	0.157 ± 0.014	1.136 ± 0.039
	1000	–	0.021 ± 0.002	0.438 ± 0.073
	3000	–	0.023 ± 0.002	0.441 ± 0.250
βCD-BA-TiO_2	250	3.677 ± 0.416	0.418 ± 0.163	1.065 ± 0.108
	500	2.423 ± 0.299	0.190 ± 0.017	1.269 ± 0.040
	1000	3.213 ± 0.168	0.114 ± 0.007	0.628 ± 0.111
	3000	−3.709 ± 1.191	0.020 ± 0.001	0.314 ± 0.096

(0.5 and 3 mg mL^{-1} of TiO_2, βCD-SA-TiO_2 and βCD-BA-TiO_2 NPs). The ones on FSC intensity are shown in the **Supplementary material, Fig. A.4-A.6.** On the other hand, to determine the metabolic activity of ATCC 25922 and ATCC 43300 under NPs treatment, cells were labelled with CDCF and fluorescence was measured. The histograms on CDCF intensity (log scale) for both bacteria are shown in Fig. 4. In addition, Fig. 5 quantifies the effect of the various NPs types and concentrations on the SSC parameters and CDCF oxidation values after 12 h incubation.

Changes in FSC and SSC intensities are represented by left and right displacement of populations. A rightward shift generally suggests larger or more internally complex particles, while a leftward shift indicates smaller or less complex particles. Additionally, the area under the curve provides insights into the total quantity of particles within a population. Variations on the FSC intensity, regarding both bacteria, were negligible and comparable to that of the control group, even at the highest dose (see **Supplementary material Fig. A.4-A.6**). That is, there was not a notable impact on *E. coli* and *S. aureus* cellular size after exposure to NPs. Some authors have previously reported an increase in FSC intensity when subjecting bacteria to NPs treatment, which they related to the easily agglomeration of nanomaterials [30,31]. In our study, in order to avoid NPs agglomeration, a voltage pulse was applied just before measuring.

Fig. 3 shows a noticeable increase in mean intensity of SSC (log scale) in both *E. coli* and *S. aureus* as the amount of TiO_2 NPs increased, suggesting that the internalization of TiO_2 NPs is related to their concentration. There was a 10-fold increase in SSC between the control sample and the 3 mg mL^{-1} TiO_2 treatment (Fig. 5). However, treatments with cyclodextrin-modified TiO_2 NPs did not show significant variations in the SSC intensity in *E. coli* with respect to the untreated control, indicating that nanoparticles were not internalized by the bacterium at any concentration. In the case of *S. aureus*, SSC intensity varied under modified NPs treatment. Thus, the high concentration of 3 mg mL^{-1} of modified NPs encapsulating sorbic acid and benzoic acid induced 2.6 and 3.2- fold increases, respectively. In a recent study, Yuan et al. also observed a significant increase in the SSC intensity when increasing the concentration of TiO_2 NPs against *E. coli* multidrug resistant LM13 strain and a standard sensitive strain ATCC 25922 [32].

On the other hand, changes in CDCF intensity staining *E. coli* and *S. aureus* were experienced due to NPs exposition (Fig. 4). In the case of *E. coli* at the highest dose of 3 mg mL^{-1} TiO_2, βCD-SA-TiO_2 and βCD-BA-TiO_2 NPs, CDCF intensity decreased by 4-times, 3-times and 4-times, respectively. Whereas, regarding *S. aureus*, the decrease was moderately lower: 2-, 3- and 1.7-times, respectively.

CDCF is a common probe used for measuring cellular H_2O_2, produced in the mitochondrial respiratory chain. The mechanism involves cell-permeable CDCF diffusion into cells, further deacetylation by cellular esterases to generate 2′,7′-dichlorodihydrofluorescein, and rapidly oxidation to 2′,7′-dichlorofluorescein, which is highly fluorescent [33,34]. So on, a decrease in the intensity of this fluorochrome implies that the metabolic activity of the bacteria diminishes. On the other hand, TiO_2 NPs are able to produce reactive oxygen species (ROS), such as hydroxyl radicals (OH•) and superoxide radicals (O_2^-) under UV irradiation. However, during the experiment, samples were not exposed to UV irradiation, and thus, the formation of ROS species by the NPs was not substantial with respect to the decrease in the metabolic activity of the bacteria caused by the several treatments. Moreover, previous researches have demonstrated that ROS such as hydroxyl radicals or hydroperoxides, can also oxidize CDCF, but with largely lower sensitivity than that of H_2O_2 [35].

When comparing the effects against *E. coli* and *S. aureus*, it can be stated that they have similar tolerance to modified and unmodified TiO_2 NPs. The overall results show that NPs may damage the cell membrane structure of both bacteria and reduce their metabolic activity. These results support those obtained through bacterial growth curves and kinetic parameters assay, and lead to conclude that all the treatments (modified and unmodified NPs) affect the viability of both *E. coli* and

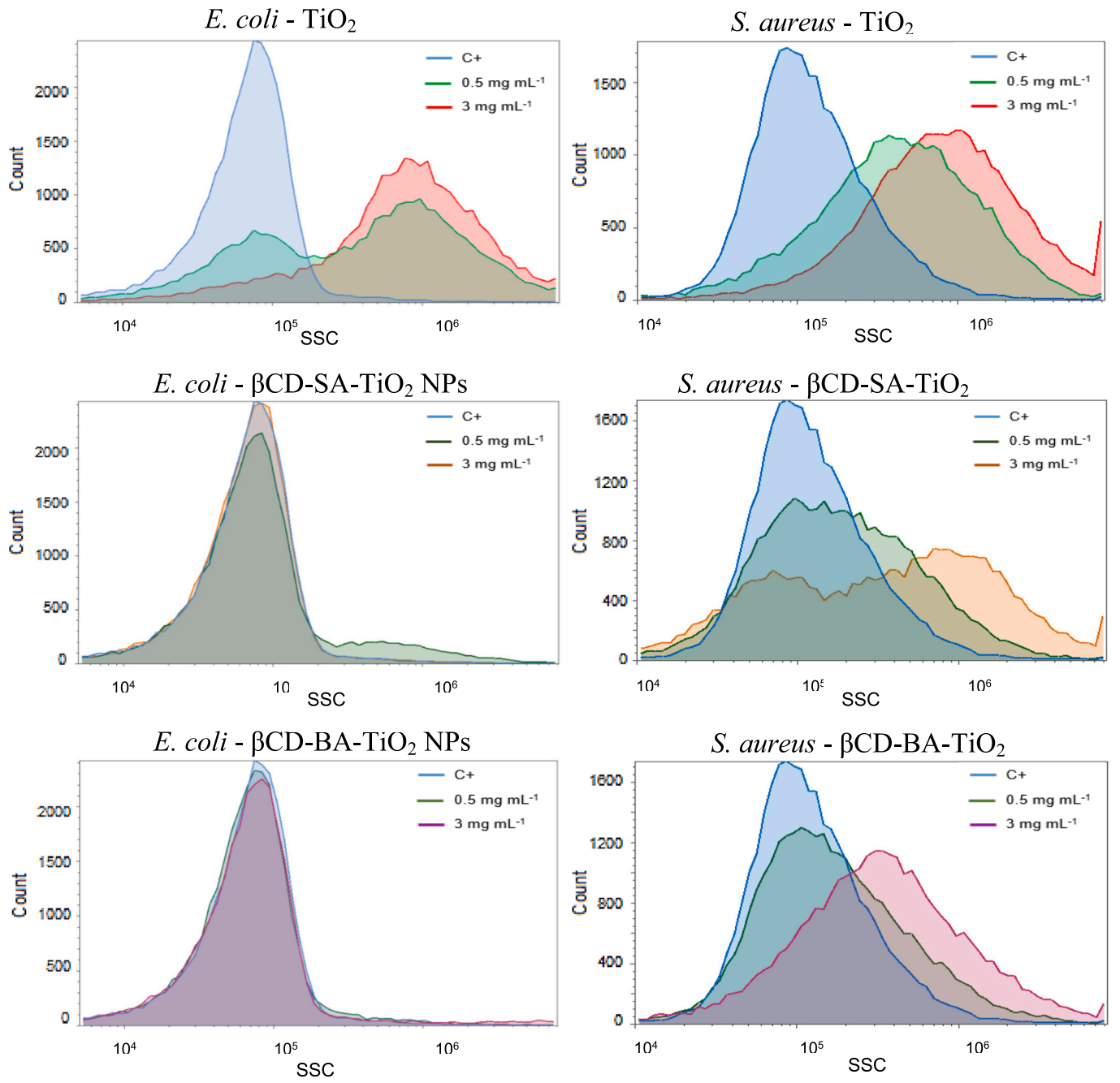

Fig. 3. Histograms of SSC values (log scale) obtained by flow cytometry of *Escherichia coli* ATCC 25922 and *Staphylococcus aureus* ATCC 43300 treated with 0.5 and 3 mg mL^{-1} concentrations of TiO_2, βCD-SA-TiO_2, and βCD-BA-TiO_2 NPs. C+ refers to the bacteria untreated with NPs. The experiment was carried out in triplicate; these curves represent one of the assays as an example.

S. aureus strains. TiO_2 NPs play the main role in the inhibitory effect of *E. coli* and *S. aureus* growth, as the most effective antibacterial treatment was the unmodified TiO_2 NPs. Higher doses of modified NPs including food preservatives were required to achieve the same bacterial inhibition. Previous researches have proposed a bimodal mechanism of action of TiO_2 NPs for bacteria inhibition (for both Gram-positive and Gram-negative bacteria), which involves NPs interaction and depolarization of the cell membrane through chemical interactions (ROS species, dissolved ions), and physical interactions (internalization of NPs or electrostatic effect), and further loss of cell viability [36]. On the other hand, the classic weak acid theory ascribed the antibacterial effect of these organic acids to the undissociated form, which can diffuse across the cell membrane and cause the acidification of the cytoplasm. However, in addition to the membrane permeability and cytoplasm acidification, there are other factors that need to be considered to fully understand their mechanism of action. Weak acids may have different targets in the cell, such as cell membrane integrity (cytoplasmic membrane for Gram-positive bacteria; outer and inner membranes for Gram-negative), synthesis of nucleic acid and proteins, and activity of crucial enzymes and osmotic homeostasis [27].

3.3. Photocatalytic activity

Photocatalytic assays were performed under two UV-A irradiation intensities (0.2 and 0.6 mW cm^{-2}) on TiO_2, βCD-BA-TiO_2 and βCD-SA-TiO_2 NPs, in order to determine how the cyclodextrin modification can

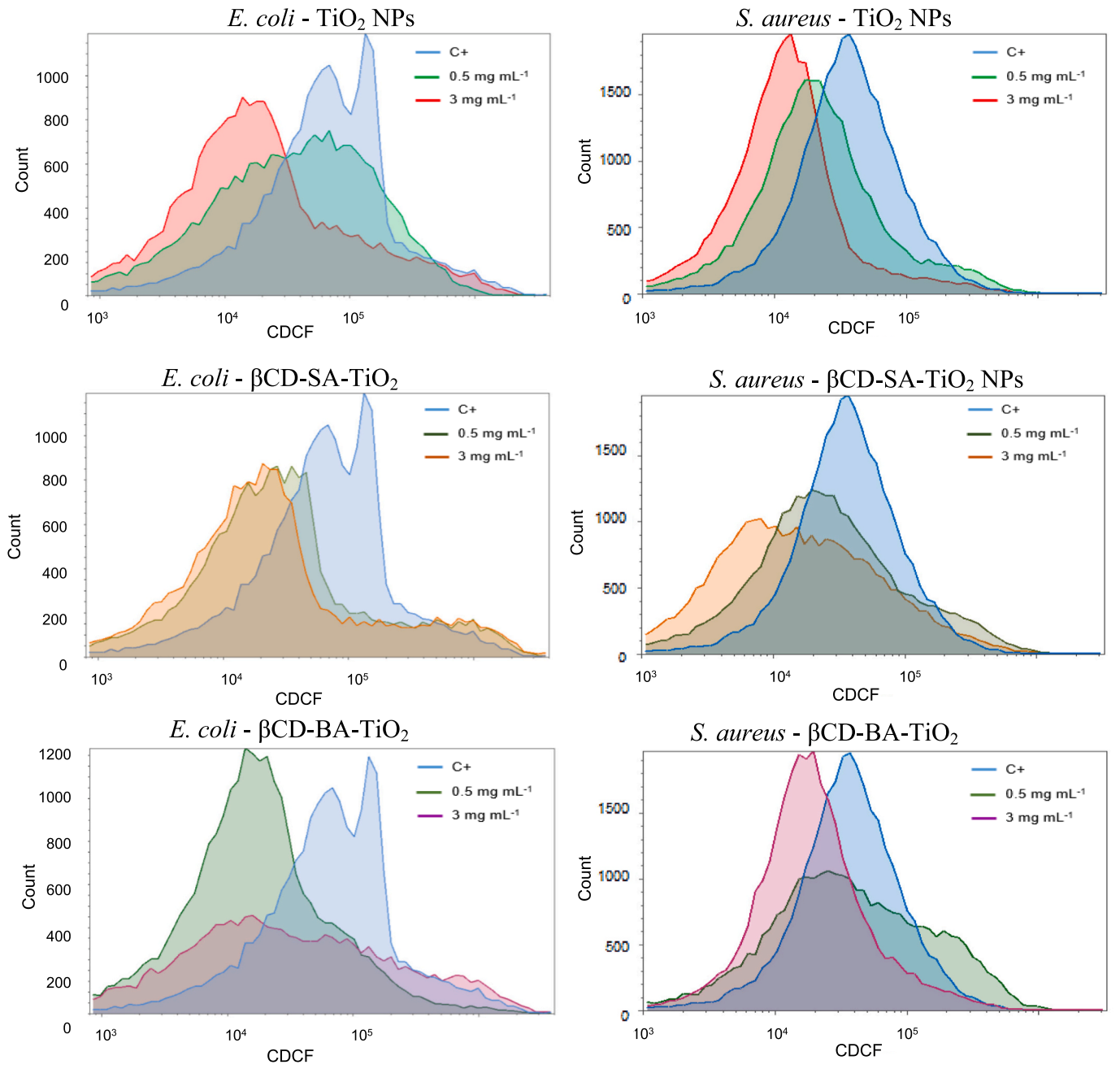

Fig. 4. Histograms of CDCF values (log scale) obtained by flow cytometry of stained *Escherichia coli* ATCC 25922 and *Staphylococcus aureus* ATCC 43300 treated with 0.5 and 3 mg mL^{-1} concentrations of TiO_2, βCD-SA-TiO_2, and βCD-BA-TiO_2 NPs. C+ refers to the bacteria untreated with NPs. The experiment was carried out in triplicate; these curves represent one of the assays as an example.

affect the photocatalytic activity of TiO_2. Methylene blue dye (MB) was used to assess the photocatalytic capacity of the different NPs. As irradiation time increased, the absorption peak at 664 nm decreased, indicating that the concentration of MB in the solution was being steadily reduced. Fig. 6 shows the degradation curves of MB, in presence of unmodified TiO_2, βCD-BA-TiO_2 and βCD-SA-TiO_2 NPs. Kinetic constants, k_{UV}, were obtained by data fitting to pseudo-first order kinetic model (Eq.2) [37]. The k_{UV} values are collected in **Table A.3** (**Supplementary material**).

The photocatalytic behaviour of βCD-BA-TiO_2 and βCD-SA-TiO_2 NPs was found very similar. Thus, and as expected, the preservative included in the βCD-TiO_2 NPs had a negligible effect in the photodegradation performance of modified NPs. Therefore, for comparison purposes, the differences will be stablished between unmodified TiO_2 and βCD-grafted TiO_2 NPs.

The photodegradation rate was directly proportional to the irradiation intensity for all the samples. The calculated kinetic constant, k_{UV} (min^{-1}), at 0.600 mW cm^{-2} for TiO_2 was 2.7 times higher than at the lower intensity of 0.200 mW cm^{-2} (0.033 vs. 0.012, respectively). While, in the case of the βCD-TiO_2 NPs the kinetic rate raised around 2.3 times with light intensity.

TiO_2 NPs exhibited higher MB degradation efficiency than βCD-modified TiO_2 NPs. At the highest irradiation intensity, TiO_2 NPs reached maximum dye degradation of 95% after 150 min. In contrast, βCD-TiO_2 NPs showed 3 times lower kinetic constant, being able to photodegrade MB dye up to 50% after 150 min (0.6 mW cm^{-2} irradiation intensity). There might be two reasons to explain this outcome. On one hand, the βCD coating on TiO_2 NPs surface can hinder their light

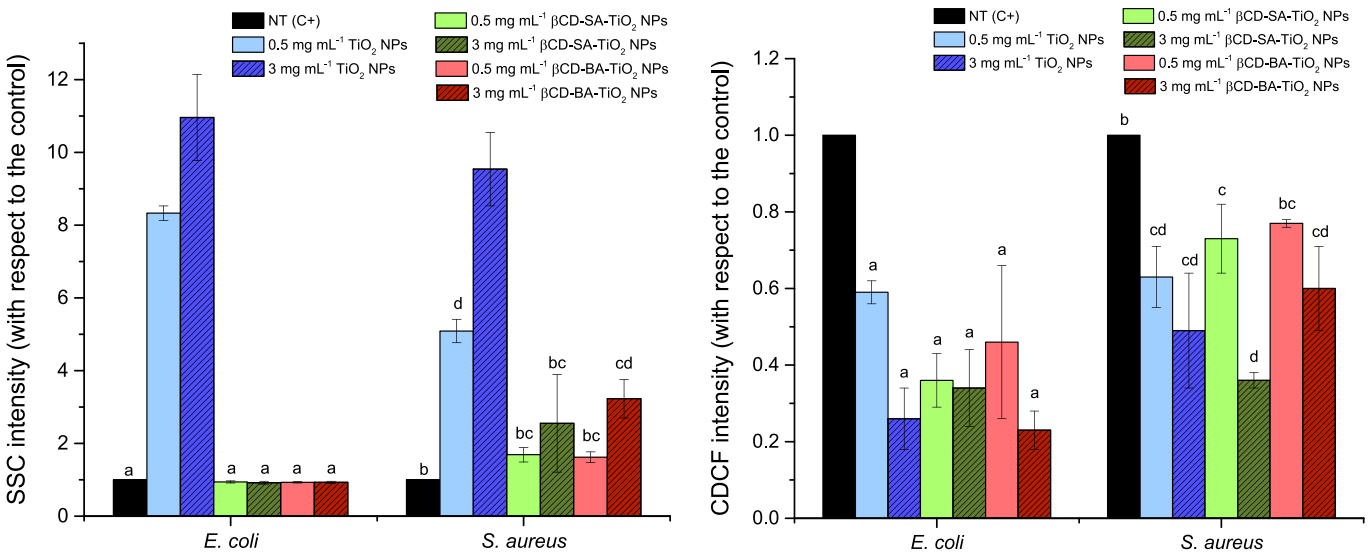

Fig. 5. Effect of TiO_2, βCD-Sorbic acid-TiO_2 and βCD-Benzoic acid-TiO_2 NPs concentrations (0.5 and 3 mg mL^{-1}) on the internal complexity (SSC) and metabolic activity (CDCF) values of *Escherichia coli* and *Staphylococcus aureus* with respect to the untreated control (NT - C+) obtained by flow cytometry. Data presented as mean ($n = 3$) ± S.D. Bars with no letters in common are significantly different ($P < 0.05$).

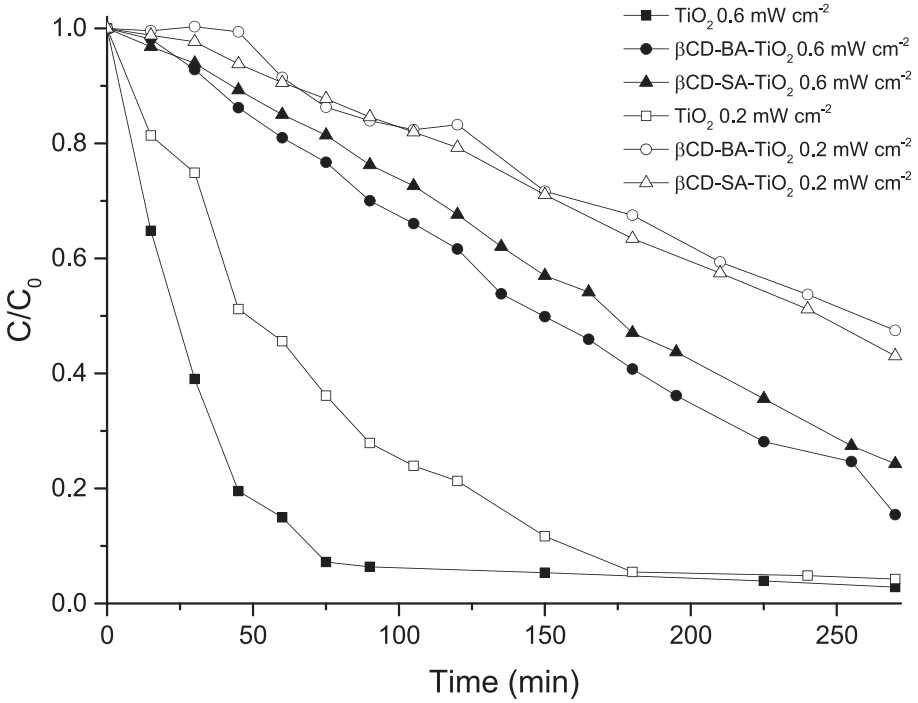

Fig. 6. Methylene blue photocatalytic degradation by TiO_2, βCD-BA-TiO_2 and βCD-SA-TiO_2 NPs as a function of time under UV light irradiation (0.2 and 0.6 mW cm^{-2}). (For interpretation of the references to color in this figure legend, the reader is referred to the web version of this article.)

absorption, and so on their photocatalytic capacity. On the other hand, the catalyst surface on βCD-TiO_2 NPs is less accessible to dye contact and degradation. These two facts caused a decrease in TiO_2 photocatalytic activity when grafting CDs. Other authors have reported similar kinetic constant values of photoinduced catalytic degradation of MB by unmodified TiO_2. Singh & Mehata in 2020 reported a rate constant value of 0.01971 min^{-1} for undoped anatase TiO_2 under 365 nm irradiation at 0.9 mW cm^{-2} intensity. However, in their research, 1 wt% transition metal ions (Ni^{2+}, Ag^{+} and Cu^{2+}) doped TiO_2 allowed to increase the photocatalytic activity of the NPs, especially the last one, achieving a 0.06022 min^{-1} rate constant value for Cu^{2+} doped TiO_2 [23]. Saroha et al. recently reported a similar reaction rate constant of 0.025 min^{-1} for untreated TiO_2 nanofibers, achieved after stimulating them with a 410 nm pump at 1 mW power, a result consistent with our own findings. Additionally, the introduction of Ag and Au NPs into the TiO_2 matrix led to substantial enhancements, with rate constants increasing by 32% and 72%, respectively [38].

The results of this work are consistent with those obtained on the antimicrobial assays, and exhibited that, high photocatalytic activities are directly related to high antibacterial capacity. In a recent study, Yong et al., [39] investigated the inactivation of *S. aureus* and *E. coli O157:H7* by using various TiO_2-based photocatalysts and light wavelengths, and concluded that the inactivation efficiency is related to the photocatalytic effects and depends on the wavelength and intensity of

the irradiation source.

4. Conclusions

TiO_2 nanoparticles (NPs) have been modified with β-cyclodextrin (βCD) and loaded with sorbic acid (SA) and benzoic acid (BA) as food preservatives in the aim of exploring new active compounds to be included in food packaging materials. *Escherichia coli* and *Staphylococcus aureus* bacteria were negatively affected in the presence of TiO_2, βCD-SA-TiO_2 and βCD-BA-TiO_2 NPs in a dose-dependent manner. Higher doses of treatment resulted in greater inhibition of bacterial growth, slower growth kinetics, larger structure cell damages and lower metabolic activity of bacteria. TiO_2 NPs were highly effective against *E. coli* and *S. aureus*, whereas relatively high concentrations of βCD-food preservative-TiO_2 NPs were required to inhibit bacterial growth. The βCD coverage on TiO_2 NPs surface may hindrance their interaction with bacteria, and thus their antibacterial activity. However, the main interest of NPs modification is found in the sustained release of the food preservatives from the cavity of the βCD, that allows to extend the antimicrobial effect over time. The overall results showed a correlation between the photocatalytic activity of the NPs, and their antibacterial capacity; high photocatalytic activities induced high antibacterial behaviour. Future studies will be performed to test the effectiveness of the different systems when incorporated as an additive into polymeric binders, and used on real food packaging applications.

Authors statement

L.G-C: Conceptualization, Methodology, Formal analysis, Investigation and experiment performance, Writing-original draft preparation, Writing-review & editing the manuscript. P.R-V: Methodology, Analysis, Investigation. C.G: Conceptualization, Methodology, Analysis, Review&editing the manuscript, Supervision. I.V: Conceptualization, Investigation, Methodology, Formal analysis, Writing-review&editing, Project administration, Funding acquisition.

Declaration of Competing Interest

The authors declare that they have no known competing financial interests or personal relationships that could have appeared to influence the work reported in this paper.

Data availability

Data will be made available on request.

Acknowledgements

The authors wish to thank the financial support provided by Gobierno de Navarra, Spain (Project OPMATNAN PI017). L.G-C. gratefully acknowledges the Asociación de Amigos de la Universidad de Navarra for her doctoral grant.

Appendix A. Supplementary data

Supplementary data to this article can be found online at https://doi.org/10.1016/j.colcom.2023.100747.

References

[1] W. Zhang, J.W. Rhim, Titanium dioxide (TiO_2) for the manufacture of multifunctional active food packaging films, Food Packag. Shelf Life 31 (2022), 100806, https://doi.org/10.1016/j.fpsl.2021.100806.
[2] M.V. Nikolic, Z.Z. Vasiljevic, S. Auger, J. Vidic, Metal oxide nanoparticles for safe active and intelligent food packaging, Trends Food Sci. Technol. 116 (2021) 655–668, https://doi.org/10.1016/j.tifs.2021.08.019.
[3] M. Alizadeh Sani, M. Maleki, H. Eghbaljoo-Gharehgheshlaghi, A. Khezerlou, E. Mohammadian, Q. Liu, S.M. Jafari, Titanium dioxide nanoparticles as multifunctional surface-active materials for smart/active nanocomposite packaging films, Adv. Colloid Interf. Sci. 300 (2022), 102593, https://doi.org/10.1016/j.cis.2021.102593.
[4] P. Kodithuwakku, D.R. Jayasundara, I. Munaweera, R. Jayasinghe, T. Thoradeniya, M. Weerasekera, P.M. Ajayan, N. Kottegoda, A review on recent developments in structural modification of TiO_2 for food packaging applications, Prog. Solid State Chem. 67 (2022), 100369, https://doi.org/10.1016/j.progsolidstchem.2022.100369.
[5] U.S. Food and Drug Administration (FDA), CFR - Code of Federal Regulations Title 21, 2020.
[6] Z. Yu, W. Wang, L. Sun, F. Kong, M. Lin, A. Mustapha, Preparation of cellulose nanofibril/titanium dioxide nanoparticle nanocomposites as fillers for PVA-based packaging and investigation into their intestinal toxicity, Int. J. Biol. Macromol. 156 (2019) 1174–1182, https://doi.org/10.1016/j.ijbiomac.2019.11.153.
[7] M. Alizadeh Sani, M. Tavassoli, S.A. Salim, M. Azizi-lalabadi, D.J. McClements, Development of green halochromic smart and active packaging materials: TiO_2 nanoparticle- and anthocyanin-loaded gelatin/κ-carrageenan films, Food Hydrocoll. 124 (2022), 107324, https://doi.org/10.1016/j.foodhyd.2021.107324.
[8] P. Ezati, Z. Riahi, J.W. Rhim, CMC-based functional film incorporated with copper-doped TiO_2 to prevent banana browning, Food Hydrocoll. 122 (2022), 107104, https://doi.org/10.1016/j.foodhyd.2021.107104.
[9] A. Buzarovska, A. Grozdanov, Biodegradable poly(L-lactic acid)/TiO_2 nanocomposites: thermal properties and degradation, J. Appl. Polym. Sci. 123 (2012) 2187–2193, https://doi.org/10.1002/app.34729.
[10] L. Goñi-Ciaurriz, G. González-Gaitano, I. Vélaz, Cyclodextrin-grafted nanoparticles as food preservative carriers, Int. J. Pharm. 588 (2020), 119664, https://doi.org/10.1016/j.ijpharm.2020.119664.
[11] G. González-Gaitano, J. Isasi, I. Vélaz, A. Zornoza, Drug carrier systems based on cyclodextrin supramolecular assemblies and polymers: present and perspectives, Curr. Pharm. Des. 23 (2017) 411–432, https://doi.org/10.2174/1381612823666161118145309.
[12] Y. Liu, D.E. Sameen, S. Ahmed, Y. Wang, R. Lu, J. Dai, S. Li, W. Qin, Recent advances in cyclodextrin-based films for food packaging, Food Chem. 370 (2022), 131026, https://doi.org/10.1016/j.foodchem.2021.131026.
[13] A. del Olmo, J. Calzada, M. Nuñez, Benzoic acid and its derivatives as naturally occurring compounds in foods and as additives: uses, exposure, and controversy, Crit. Rev. Food Sci. Nutr. 57 (2017) 3084–3103, https://doi.org/10.1080/10408398.2015.1087964.
[14] J.H.F. de Jesus, I.M. Szilágyi, G. Regdon, E.T.G. Cavalheiro, Thermal behavior of food preservative sorbic acid and its derivates, Food Chem. 337 (2021), 127770, https://doi.org/10.1016/j.foodchem.2020.127770.
[15] L. Behera, B. Barik, S. Mohapatra, Improved photodegradation and antimicrobial activity of hydrothermally synthesized 0.2Ce-TiO_2/RGO under visible light, Colloids Surfaces A Physicochem. Eng. Asp. 620 (2021), 126553, https://doi.org/10.1016/j.colsurfa.2021.126553.
[16] F. Chen, X. Yang, F. Xu, Q. Wu, Y. Zhang, Correlation of photocatalytic bactericidal effect and organic matter degradation of TiO_2 part I : observation of phenomena, Environ. Sci. Technol. 43 (2009) 1180–1184, https://doi.org/10.1021/es802499t.
[17] P. Phuinthiang, Y. Mingmongkol, D. Channei, A. Nakaruk, Visible-light-driven photodegradation of methylene blue dye and visible-light-driven photodegradation of methylene blue dye and pathogenic *Escherichia Coli* by Mn-doped TiO_2 nanoparticles, Nano Br. Rep. Results 18 (2023) 2350043, https://doi.org/10.1142/S1793292023500431.
[18] M.E. Owda, A.S. Elfeky, R.E. Abouzeid, A.K. Saleh, M.A. Awad, H.A. Abdellatif, F. M. Ahmed, A.S. Elzaref, Enhancement of photocatalytic and biological activities of chitosan/ activated carbon incorporated with TiO_2 nanoparticles, Environ. Sci. Pollut. Res. 29 (2022) 18189–18201, https://doi.org/10.1007/s11356-021-17019-y.
[19] R.H. Rosa, R.S. Silva, L.L. Nascimento, M.H. Okura, A.O.T. Patrocinio, A. Rossignolo, Photocatalytic and antimicrobial activity of TiO_2 films deposited on fiber-cement surfaces, Catalysts. 13 (2023) 1–14, https://doi.org/10.3390/catal13050861.
[20] D. Zhang, H. Hu, J. An Wei, X. Xu, L. Chen, X. Wu, Q. Yu, B. Xing Zhang, L. G. Wang, Zr-doped TiO_2 ceramic nanofibrous membranes for enhancing photocatalytic organic pollutants degradation and antibacterial activity, Colloids Surfaces A Physicochem. Eng. Asp. 665 (2023), 131231, https://doi.org/10.1016/j.colsurfa.2023.131231.
[21] L. Goñi-Ciaurriz, I. Vélaz, Antibacterial and degradable properties of β -cyclodextrin-TiO_2 cellulose acetate and polylactic acid bionanocomposites for food packaging, Int. J. Biol. Macromol. 216 (2022) 347–360, https://doi.org/10.1016/j.ijbiomac.2022.06.202.
[22] W.E. Garthright, Refinements in the prediction of microbial growth curves, Food Microbiol. 8 (1991) 239–248, https://doi.org/10.1016/0740-0020(91)90056-8.
[23] M.K. Singh, M.S. Mehata, Enhanced photoinduced catalytic activity of transition metal ions incorporated TiO_2 nanoparticles for degradation of organic dye: absorption and photoluminescence spectroscopy, Opt. Mater. (Amst). 109 (2020), 110309, https://doi.org/10.1016/j.optmat.2020.110309.
[24] L. Goñi-Ciaurriz, M. Senosiain-Nicolay, I. Vélaz, Aging studies on food packaging films containing β-cyclodextrin-grafted TiO_2 nanoparticles, Int. J. Mol. Sci. 22 (2021) 1–13, https://doi.org/10.3390/ijms22052257.
[25] R. Capita, M. Vicente-Velasco, C. Rodríguez-Melcón, C. García-Fernández, J. Carballo, C. Alonso-Calleja, Effect of low doses of biocides on the antimicrobial resistance and the biofilms of *Cronobacter sakazakii* and *Yersinia enterocolitica*, Sci. Rep. 9 (2019) 1–12, https://doi.org/10.1038/s41598-019-51907-1.

[26] H.J. Lu, F. Breidt, I.M. Pérez-Díaz, J.A. Osborne, Antimicrobial effects of weak acids on the survival of *Escherichia coli* O157:H7 under anaerobic conditions, J. Food Prot. 74 (2011) 893–898, https://doi.org/10.4315/0362-028X.JFP-10-404.

[27] U. Kanjee, W.A. Houry, Mechanisms of acid resistance in enterohemorrhagic *Escherichia coli*, Annu. Rev. Microbiol. 67 (2013) 65–81, https://doi.org/10.1146/annurev-micro-092412-155708.

[28] Q. Wei, X. Wang, J.H. Cheng, G. Zeng, D.W. Sun, Synthesis and antimicrobial activities of novel sorbic and benzoic acid amide derivatives, Food Chem. 268 (2018) 220–232, https://doi.org/10.1016/j.foodchem.2018.06.071.

[29] V.K. Yemmireddy, Y.C. Hung, Effect of binder on the physical stability and bactericidal property of titanium dioxide (TiO_2) nanocoatings on food contact surfaces, Food Control 57 (2015) 82–88, https://doi.org/10.1016/j.foodcont.2015.04.009.

[30] M. Ghosh, M.J.S. Sinha, A. Chakraborty, S.K. Mallick, M. Bandyopadhyay, A. Mukherjee, *In vitro* and *in vivo* genotoxicity of silver nanoparticles, Mutat. Res. Genet. Toxicol. Environ. Mutagen. 749 (2012) 60–69, https://doi.org/10.1016/j.mrgentox.2012.08.007.

[31] R.G. Combarros, S. Collado, M. Díaz, Toxicity of titanium dioxide nanoparticles on *pseudomonas putida*, Water Res. 90 (2016) 378–386, https://doi.org/10.1016/j.watres.2015.12.040.

[32] W. Yuan, Y. Wei, Y. Zhang, L. Riaz, Q. Yang, Q. Wang, R. Wang, Resistance of multidrug resistant *Escherichia coli* to environmental nanoscale TiO_2 and ZnO, Sci. Total Environ. 761 (2021), 144303, https://doi.org/10.1016/j.scitotenv.2020.144303.

[33] H.R. McLennan, M.D. Esposti, The contribution of mitochondrial respiratory complexes to the production of reactive oxygen species, J. Bioenerg. Biomembr. 32 (2000) 153–162, https://doi.org/10.1023/A:1005507913372.

[34] X. Chen, Z. Zhong, Z. Xu, L. Chen, Y. Wang, 2′,7′-Dichlorodihydrofluorescein as a fluorescent probe for reactive oxygen species measurement: forty years of application and controversy, Free Radic. Res. 44 (2010) 587–604, https://doi.org/10.3109/10715761003709802.

[35] C. Yang, L. Jiang, H. Zhang, L.A. Shimoda, R.J. Deberardinis, G.L. Semenza, Analysis of Hypoxia-Induced Metabolic Reprogramming, 1st ed, Elsevier Inc., 2014, pp. 425–455, https://doi.org/10.1016/B978-0-12-416618-9.00022-4.

[36] Y.N. Slavin, J. Asnis, U.O. Häfeli, H. Bach, Metal nanoparticles: understanding the mechanisms behind antibacterial activity, J. Nanobiotechnol. 15 (2017) 1–20, https://doi.org/10.1186/s12951-017-0308-z.

[37] M.K. Singh, M.S. Mehata, Phase-dependent optical and photocatalytic performance of synthesized titanium dioxide (TiO_2) nanoparticles, Optik. 193 (2019), 163011, https://doi.org/10.1016/j.ijleo.2019.163011.

[38] S. Jyoti, E. Rany, M. Devi, P. Pathi, M. Kumar, S.N. Sharma, Plasmon-assisted photocatalysis of organic pollutants by Au/Ag-TiO_2 nanocomposites: a comparative study, Mater. Today Sustain. 23 (2023), 100466, https://doi.org/10.1016/j.mtsust.2023.100466.

[39] S.S. Yong, J.I. Lee, D.H. Kang, TiO_2-based photocatalyst generated reactive oxygen species cause cell membrane disruption of *Staphylococcus aureus* and *Escherichia coli* O157:H7, Food Microbiol. 109 (2022), 104119, https://doi.org/10.1016/j.fm.2022.104119.